Accepted Manuscript

International Journal of Pattern Recognition and Artificial Intelligence

Article Title:	Error Analysis and Compensation in Images stitching for the Mechanically Stitched CCD Aerial Cameras
Author(s):	Haipeng Kuang, Lina Zheng, Guoqin Yuan, Jianjun Sun, Zhuang Zhang
DOI:	10.1142/S0218001419550127
Received:	01 October 2018
Accepted:	04 December 2018
To be cited as:	Haipeng Kuang *et al.*, Error Analysis and Compensation in Images stitching for the Mechanically Stitched CCD Aerial Cameras, *International Journal of Pattern Recognition and Artificial Intelligence*, doi: 10.1142/S0218001419550127
Link to final version:	https://doi.org/10.1142/S0218001419550127

Error Analysis and Compensation in Images stitching for the Mechanically Stitched CCD Aerial Cameras

Haipeng Kuang,
Key Laboratory of Airborne Optical Imaging and Measurement, Changchun Institute of Optics, Fine Mechanics and Physics, Chinese Academy of Science, Changchun, China, 130033
kuanghp@163.com
Lina Zheng*
Key Laboratory of Airborne Optical Imaging and Measurement, Changchun Institute of Optics, Fine Mechanics and Physics, Chinese Academy of Science, Changchun, China, 130033
ailsazheng@163.com
Guoqin Yuan
Key Laboratory of Airborne Optical Imaging and Measurement, Changchun Institute of Optics, Fine Mechanics and Physics, Chinese Academy of Science, Changchun, China, 130033
13943195584@139.com
Jianjun Sun
Key Laboratory of Airborne Optical Imaging and Measurement, Changchun Institute of Optics, Fine Mechanics and Physics, Chinese Academy of Science, Changchun, China, 130033
jianjun_sun@163.com
Zhuang Zhang
Jilin Wancheng Co.Ltd, Changchun, China, 130033
hhu1990_zhuagn@163.com

Abstract：Image misalignment during image stitching is a common issue for the mechanically stitched CCDs in the aerial cameras due to the relative image motion between CCDs. In this paper, we analyze the error in imaging stitching for the mechanically stitched CCDs and propose a compensation method based on position and orientation system (POS). Firstly, the imaging relationship of overlapping pixels in mechanical stitching is analyzed. The imaging model of adjacent CCD is constructed according to the collinear equation. The effects of stitching staggered distance, carrier attitude change and flight speed on the image mosaic of overlapping areas are given. Monte Carlo algorithm is used to analyze the statistical value of image mosaic error in overlapping area under typical working conditions. Then, a geometric correction method based on POS recording of external orientation elements of adjacent CCD imaging is proposed. The overlapping area stitching error is reduced from 14.9 pixels to 0.4 pixels which meets the engineering requirements. The mechanical stitching mathematical model, analysis and correction method established in this paper have strong engineering and application significance for mechanical stitching of aerial cameras.

Keywords：mechanically stitched CCD; error analysis; aerial camera; POS-assisted geometric correction

1. Introduction

Aerial cameras have extremely important applications on military reconnaissance[1], resource exploration[2], surveying and mapping[3] etc. The large field of view (FOV) has always been an important development direction for aerial cameras and is a direct way to obtain ground information as efficiently as possible[4-6]. However, as the camera's FOV increases, the length of the detector required for imaging is also increasing, which is far beyond the length of a single CCD on the market[7-9]. Multiple CCD combinations are needed to increase the focal plane length, that is, the CCD stitching.

Mechanical stitching is a common stitching method. It is a form of CCD stitching into a 2-line staggered parallel array on the focal plane of the camera. It has the advantages of compact structure, no additional chromatic aberration, simple focal plane, etc[10-11]. In order to avoid the occurrence of sag between different CCDs' FOV due to factors such as aircraft attitude changes, a certain number of overlapping pixels are usually kept between adjacent CCDs. When the camera is operating, the overlapping pixels image the ground scene independently, and the images of the adjacent two CCDs can be stitched according to the image of the same scene in the overlapping area to form a larger image. High-resolution optical cameras in commercial satellites such as IKONOS, Quick Bird, EROS-B1 OrbView-3, and CBERS-02B use the CCD stitching method[12-13].

For mechanical stitching, multiple CCDs are staggered in the focal plane. The overlapping pixels between adjacent CCDs image the ground scene at different times, resulting in different attitude angles for the adjacent CCDs. Problems such as overlapping of image points, misalignment, etc. occur and affect image interpretation[14]. The general image stitching method is pixel stitching [15] by overlapping the same area in two images. Yu et al. [16] obtained the same scale image by using SIFT feature rough matching remote sensing image, and then extracted Harris corner points in the wavelet domain for fine matching. Bay et al. [17] proposed SURF feature detection operator, which is faster. The SURF operator is used by Li et al. [18] to perform coarse matching with the fast minimum truncated square sum estimation operator to achieve sub-pixel matching of the image. Pixel stitching is simple and the calculation is small, but it destroys the object image relationship. The stitched image loses the projection geometry and cannot produce the higher precision data products in the post processing. This paper analyzes the relationship between overlapping area of the mechanically stitched CCDs and ground scene imaging, constructs a mathematical model by using the collinear equation, analyzes the influence of aircraft attitude, CCD separation distance and other factors on image stitching, and proposes a POS assisted measurement method for image stitching, without destroying the object image relationship. It establishes coordinate transformation relationship between stitched image, object-side projection surface and original image, and establish strict coordinate mapping between stitched image and original image. High-precision image stitching is achieved by resampling the original image, and the stitched image can be directly used for the production of high-precision data products.

2. Mechanical stitching imaging model

Figure 1(a) is a schematic for two mechanically stitched CCDs. Figure 1(b) shows the projection on the ground of imaging area of both detectors. The ground scene in the overlapping area is then imaged separately in two adjacent detectors.

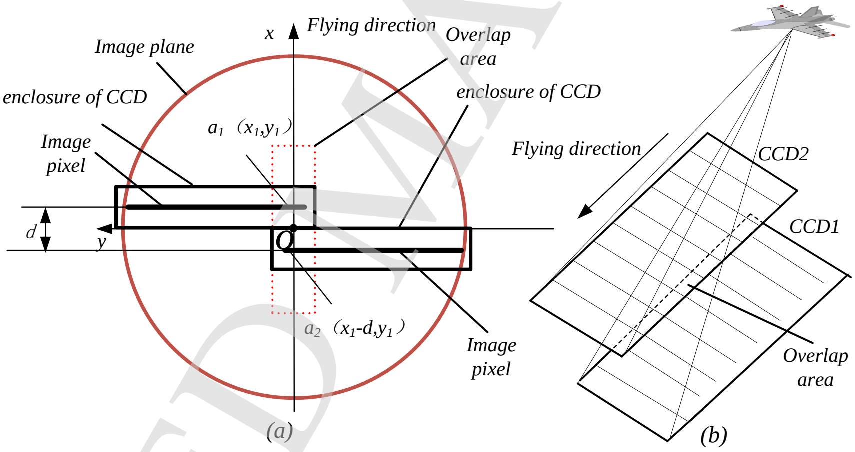

Figure 1Mechanical stitching schematic (a) geometry arrangement of two mechanically stitched CCDs, (b) scenery imagery in overlapping areas.

The image plane coordinate system *xoy* is established with the camera main point as the origin *o*, and the *y* axis is the long direction of the CCD, as shown in Fig. 1(a). The image point *y* coordinates of the adjacent two CCDs in the overlap region are the same, and the *x* coordinates are a_1, a_2 in Fig. 1, respectively. The difference between a_1 and a_2 is the detector staggering distance d. In this paper, the pixel with the same y coordinate in the overlap region is called the same-named pixel.

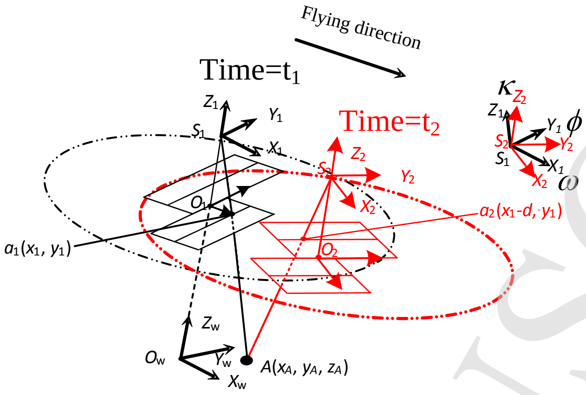

Figure 2 Schematic of the imaging process of two mechanically stitched CCDs.

The imaging process of two mechanically stitched CCDs is shown in Fig. 2. For the convenience of description, the image space coordinate system *S-XYZ* is established, in which the *X* and *Y* axes are parallel to the *xy* axes of image plane coordinate system and the directions are the same. The distance between the *XY* plane and the image *xy* plane coordinate system is the camera focal length *f*. The image space coordinate system and the image plane coordinate system move together with the aircraft. The world coordinate system O_w-$X_WY_WZ_W$ is established as a fixed coordinate, and its axes are parallel and consistent with the image space coordinate system S_1-$X_1Y_1Z_1$ at time t_1. The distance between the X_WY_W plane and the X_1Y_1 plane is the aircraft's altitude *H*. The mechanical stitching imaging process is as follows: at time=t_1, the image point a_1 in the overlap region images the ground point *A* (X_A, Y_A, Z_A) in the world coordinate system, and the aircraft flies forward, at time=t_2, the image space coordinate system is S_2-$X_2Y_2Z_2$, at this time, the image point a_2 in the overlap region is imaged by *A*, and the coordinates of the S_1-$X_1Y_1Z_1$ and S_2-$X_2Y_2Z_2$ coordinate system origins in O_w-$X_WY_WZ_W$ are *(0,0,H)* and $(V_t,0,H)$, respectively. *V* is the carrier track speed, and the coordinates of the same-named pixels a_1, $a_2$in the image plane coordinate system are (x_1, y_1), $(x_1\text{-}d, y_1)$, respectively.

According to the collinear equation[19-20], at time t_1,

$$\begin{bmatrix} x_1 \\ y_1 \\ -f \end{bmatrix} = \lambda_1^{-1} R_1^{\mathrm{T}} \begin{bmatrix} x_A \\ y_A \\ z_A - H \end{bmatrix} \tag{1}$$

In the same way, at time t_2,

$$\begin{bmatrix} x_1 - d \\ y_1 \\ -f \end{bmatrix} = \lambda_2^{-1} R_2^{\mathrm{T}} \begin{bmatrix} x_A - Vt \\ y_A \\ z_A - H \end{bmatrix} \tag{2}$$

In equations (1) and (2), λ_1, λ_2 are the shooting scale coefficients, *f* is the camera focal length, and R_1 and R_2 are the rotation matrices of S_1—$X_1Y_1Z_1$ and S_2—$X_2Y_2Z_2$ with respect to the three attitude angles $\phi-\omega-\kappa$ of the world coordinate system O_w-$X_WY_WZ_W$. Here, the attitude angles are rotated by the order of *y-x-z*. Since S_1—$X_1Y_1Z_1$ is parallel to O_w-$X_WY_WZ_W$, the attitude angle at time t_1 is $\phi_1 = \omega_1 = \kappa_1 = 0$, R_1 is the identity matrix, and the attitude angle at time t_2 is $\phi_2, \omega_2, \kappa_2$ respectively.

$$R_2 = \begin{bmatrix} \cos\varphi_2 & 0 & -\sin\phi_2 \\ 0 & 1 & 0 \\ \sin\phi_2 & 0 & \cos\phi_2 \end{bmatrix} \times \begin{bmatrix} 1 & 0 & 0 \\ 0 & \cos\omega_2 & -\sin\omega_2 \\ 0 & \sin\omega_2 & \cos\omega_2 \end{bmatrix} \times \begin{bmatrix} \cos\kappa_2 & -\sin\kappa_2 & 0 \\ \sin\kappa_2 & \cos\kappa_2 & 0 \\ 0 & 0 & 1 \end{bmatrix} \tag{3}$$

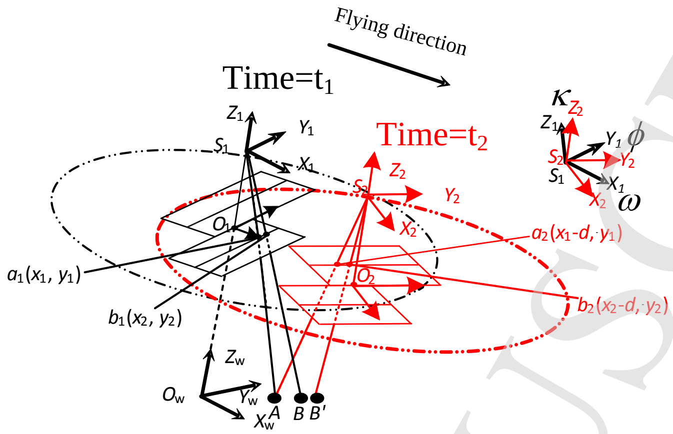

Figure 3 Schematic diagram of the stitching error of the same-named pixel caused by mechanical stitching

As shown in Fig. 3, at time=t_1, the image points a_1 and b_1 image the ground points A and B, and at time=t_2, the same-named pixel a_2 images A, but due to the change of the flight attitude of the carrier, the same-named pixel b_2 imaging point is B'. If the images of the two detectors are directly stitched according to the same-named pixel, point B will coincide with B', resulting in image misalignment.

3. Monte Carlo algorithm analyzes the influence of stitching error of the same-named pixel

According to the previous analysis, when the mechanical stitching is performed, the postures of the same-named pixel are different during exposure, resulting in problems such as misalignment, pull-over, and overlap in image stitching. In this section, the Monte Carlo algorithm is used to calculate the statistic of the stitching error of the same-named pixels by giving the error probability distribution model and working parameters of the relevant parameters[21].

According to the mathematical model established by equations (1)-(3), the three attitude angles affect the stitching error of the same-named pixel. According to the error distribution of the three attitude angles and the characteristic value, a random number sequence is generated. The three attitude angles are substituted into the error mathematical model to calculate the statistical value of the stitching error of the same-named pixel, as shown in Table 1. POS is not used in this condition. The angular stability error is 0.3 °.

Table 1 Mathematical model of the attitude angles

No.	Name	Error distribution	Unit	Root mean square value	Remark
1	Angular stability error φ	Normal distribution	deg	0.3	Angle attitude stabilizing residual
2	Angular stability error ω	Normal distribution	deg	0.3	Angle attitude stabilizing residual
3	Angular stability error κ	Normal distribution	deg	0.3	Angle attitude stabilizing residual

The camera operating parameters are as follows.

a) aircraft's altitude H =2600 m;
b) speed V = 234 km / h;
c) focal length f=81 mm;
d) ground resolution GSD=0.32 m;
e) d=44 mm;
f) 100 same-named pixels.

Image points a_1 and b_1 eleven seed points are selected in the image plane, and numerical simulation is carried out according to the initial conditions listed in Table 1 and the simulation algorithm flow established by equations (1)-(3). The simulation is repeated 500 times. Figure 4 plots the coordinates of the ground points *A*, *B* and *B'*. The root mean square of the misalignment error of *B* and *B'* is 4.78 m, which are 14.9 pixels. According to the existing experience, post image stitching will be affected when the error is larger than 1/3 pixels. Figures 5 and 6 plot the histograms of error distribution in the X and Y directions. We can conclude that the stitching error of the same-named pixels is mainly in the Y direction, which is vertical to the flight direction.

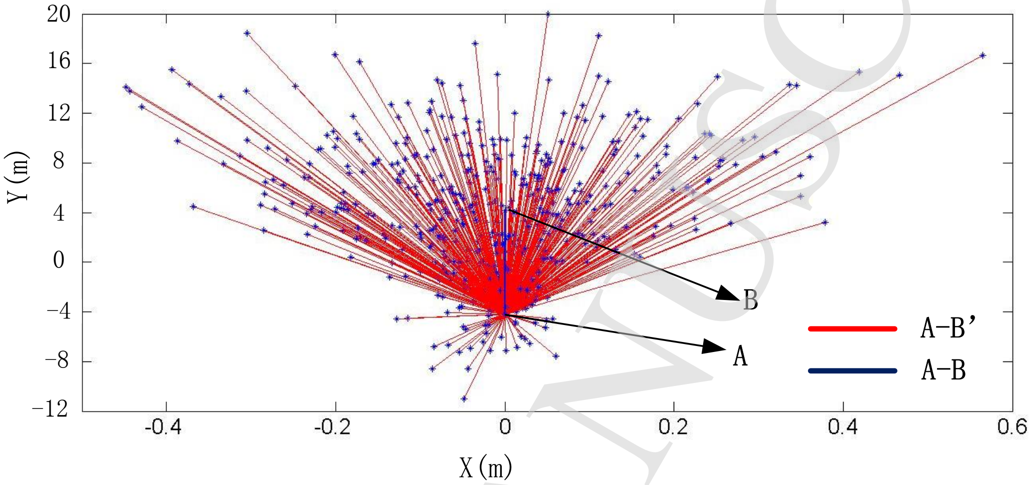

Figure 4 The coordinates corresponding to the ground points *A*, *B* and *B'*

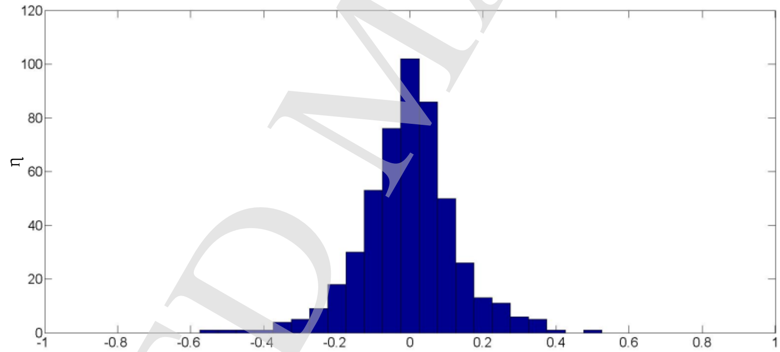

Figure 5 Histogram of error distribution in the X direction

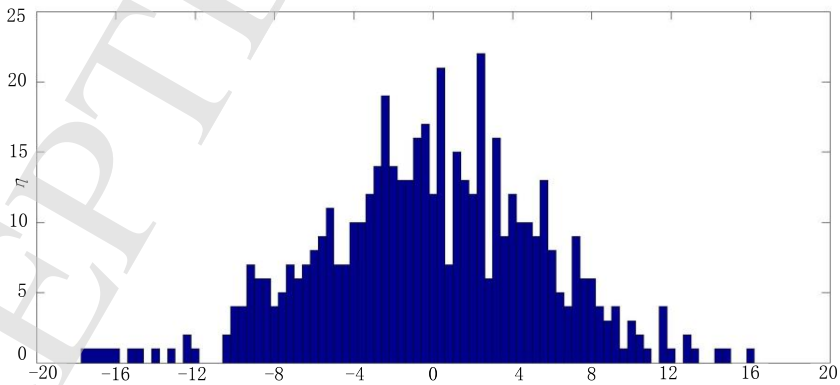

Figure 6 Histogram of error distribution in the Y direction

4. POS assisted stitching correction

At the end of the 20th century, POS combines differential GPS technology and inertial navigation (INS) technology to acquire six external orientation elements of aerial cameras during aerial photography. It can be directly applied to the correction of aerial photogrammetric image [22]. Here, POS AV610 is used to record the external orientation elements of adjacent CCD at the imaging time, and the attitude angles of the same-named pixel during imaging the ground scene. Substitute the parameters in equation (3), the rotation matrix R_2 is obtained when the overlapping region t_2 is imaged. The correction technique is applied to the image point and the position of the image point to where it is in the rotation matrix is R_1 is corrected and images are stitched. The problem of stitching mismatch of the same-named pixel caused by the attitude change is eliminated. The eventual factor affecting the stitching error of the same-named pixel is the precision of POS AV610.

When the aircraft's altitude is 2600 m, the accuracy of the three angles is measured $\phi_2 = 0.0025^0, \omega_2 = 0.0025^0, \kappa_2 = 0.005^0$. The stitching error of the same-named pixels is shown in Fig.7.

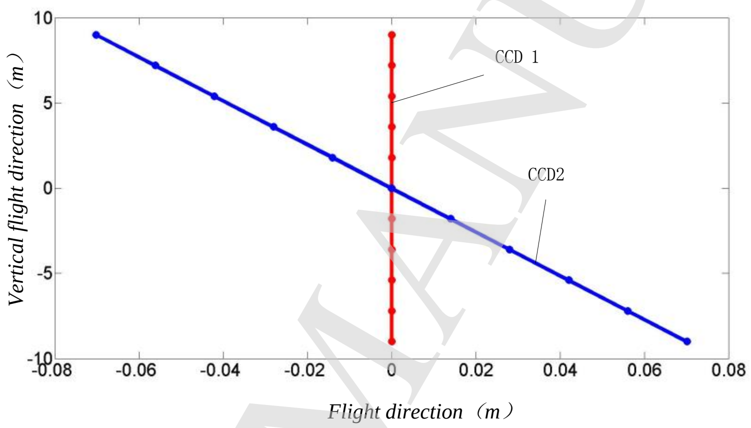

Figure 7 The stitching error of the same-named pixels with POS AV610 recording external orientation elements for correction stitching error

Considering a ground resolution of 0.32 m, the misalignment error is 0.07 m, which is about 1/4 pixel, and has no significant effect on image stitching.

5. Flight verification

The flight image of a certain type of camera with mechanical stitching is processed by the method described previously. The camera parameters are focal length f=81 mm, the number of CCD overlapping pixels is 100, and the altitude is 2600 m. The camera mounted on the aircraft is shown in Fig.8. The flight image comparison analysis is shown in Fig. 9. Figures 9(a) and 9(b) are images from two CCDs, respectively. Figure 9(c) shows when direct stitching, the misalignment error of the same-named pixels is 17.3 pixels. There is a large misalignment in the overlap region. Figure 9(d) shows the stitching after geometric correction based on the external orientation elements acquired by POS. The correct image stitching is achieved. Fig. 10 plots the histogram of error distribution of 200 same-named points in the overlapping area of stitched image.

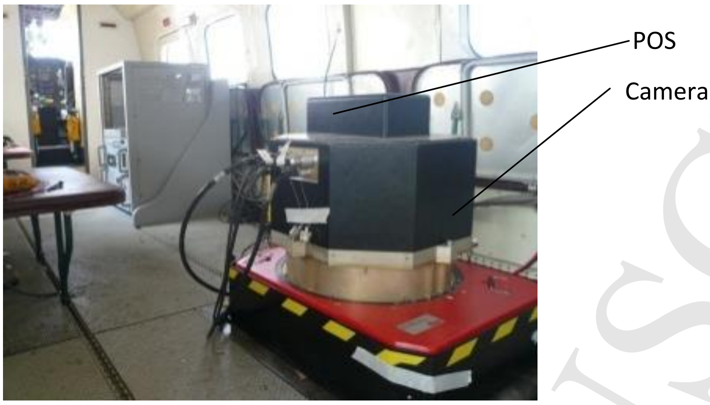

Figure 8 Camera mounted on the aircraft

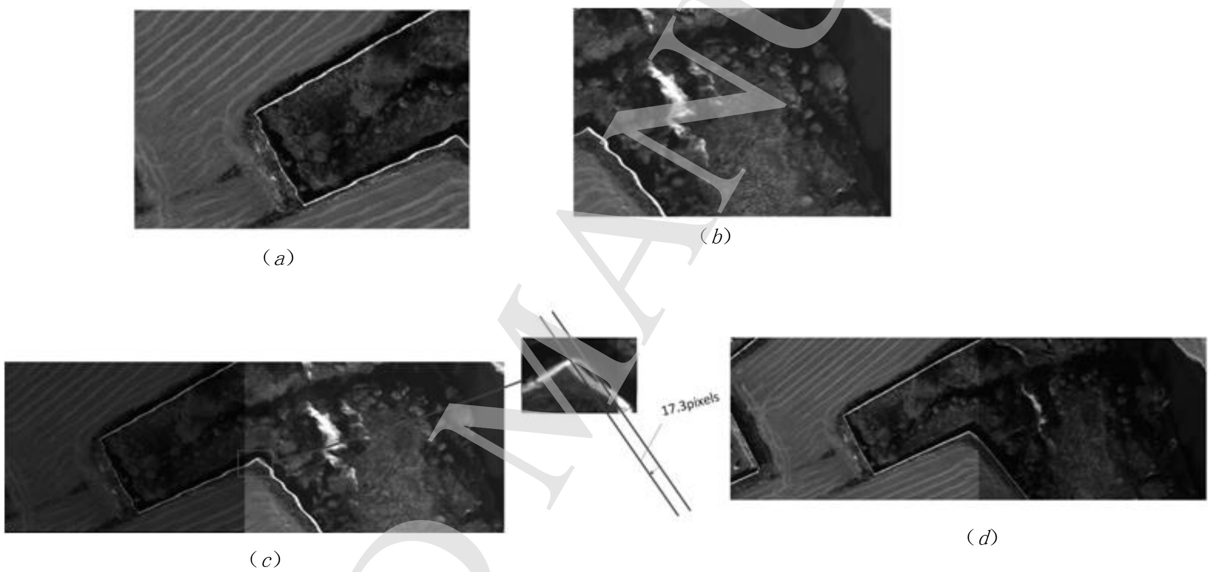

Figure 9 Flight image verification. (a)images from CCD1. (b) images from CCD2. (c) images of the two CCDs directly stitched according to the same-named pixel. (d) images of the two CCDs stitched after geometric correction based on the external orientation elements acquired by POS.

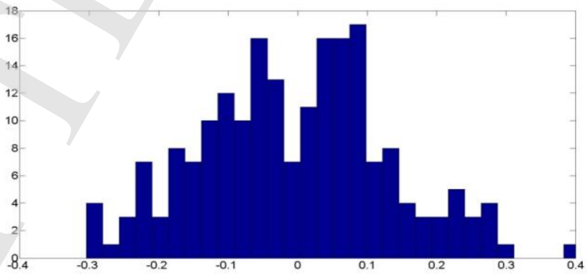

Figure 10 Histogram of error distribution of same-named points

6. Conclusion

The imaging model of adjacent mechanically stitched CCDs is constructed according to the collinear equation. Monte Carlo algorithm is used to analyze the image stitching error under typical conditions. A POS-assisted image error correction method is proposed. The numerical analysis shows that the stitching error of the overlap region is reduced from 14.9 pixels to 1/4 pixels. The actual flight image shows the stitching error is 17.3 pixels, which agrees with the numerical analysis method. The mechanical stitching mathematical model, analysis and correction method established in this paper have engineering and application significance for mechanical stitching of aerial cameras. The method is suitable not only for aerial camera, but also for remote sensing satellite.

Reference:

1. Qin Lijuan, Wang, Ting. Improved Position and Attitude Determination Method for Monocular Vision in Vehicle Collision Warning System. International Journal of Pattern Recognition and Artificial Intelligence, v 30, n7 (2016).
2. Wang, Huan. A shape-aware road detection method for aerial images. International Journal of Pattern Recognition and Artificial Intelligence, v31, n4 (2017).
3. Zheng Lina, Yuan Guoqin. Calibration Method for Mapping camera Based on a Precise Grouped Approach Method. International Journal of Pattern Recognition and Artificial Intelligence, v32, n11 (2018).
4. LÜ Hengyi，LIU Yang，GUO Yongfei. Computation of overlapping pixels of mechanical assembly CCD focal planes in remote sensing cameras. Optics Precision Engineering，20(5)：1041-1043(2012).
5. Antoni Rogalski. Progress in focal plane array technologies. Progress in Quantum Electronics，36(2-3)(2012).
6. Paul R Jorden, David G Morris, Peter J Pool. Technology of large focal planes of CCDs. Proc. SPIE，5167：72-82(2004).
7. Ning Yonghui, Guo Yongfei. Correction of pixel response non-uniformity in TCICCD mosaic camera. Chinese Optics, 6(3): 386-394(2013).
8. LIU Hailong, HAN Chenshan, LI Xiangzhi，et al. Vibration parameter measurement of TDICCD space camera with mechanical assembly. Optics Precision Engineering, 23(3):729-737(2015).
9. SUN Bin, LI Jinglin, ZHANG Xingxiang, et al. Interleaving assembly of TDICCDs on 600mm focal plan. Optics Precision Engineering, 22(11):2908-2913(2014).
10. LI Zhaohui，WANG Zhaoxun，WU Keyong. Optical assembly of CCD focal plane for space camera. Optics Precision Engineering, 8(3):213-216(2000).
11. ZHANG Xingxiang，REN Jianyue. Mechanical interleaving assembly of TDICCD focal plane. Acta Optical Sinica, 26(5):740-745(2001).
12. REN Jianyue，SUN Bin，ZHANG Xingxiang，et al. Precision measurement of TDICCD interleaving assembly. Optics Precision Engineering, 16(10):1853-1857(2008).

13. LONG Xiaoxiang，WANG Xiaoyan，ZHONG Huimin. Analysis of image quality and processing method of a space-borne focal plane view splicing TDI CCD camera. SCIENCE CHINA Information Sciences, 41(s):19-31(2011).
14. Zagrouba E, Barhoumi W, Amri S. An efficient image-mosaicing method based on multifeature matching. Machine Vision and Applications, 20(3):139-162(2009).
15. CHENG Zhenggang, ZHANG Li. An Aerial image mosaic method Based on UAV Position and Attitude Information. Acta Geodaetica et Cartographica Sinica, 45(6): 698-705(2016).
16. Yu L, Zhang D, Holden E J. A fast and fully automatic registration approach based on point features for multi-source remote-sensing images. Computers&Geosciences, 34(7): 838-848(2008).
17. BAY H, ESS A. Speeded-UP Robust Features (SURF). Computer Vision and Image Understanding, 110(3):346-359(2008).
18. Li D, Zhang Y. A fast offset estimation approach for insar image subpixel registration. IEEE Geoscience & Remote Sensing Letters, 9(2): 267-271(2012).
19. T. TOUTIN. Review article: Geometric processing of remote sensing images: models, algorithms and methods.INT. J. REMOTE SENSING, 25(10):1893–1924(2004).
20. Dejiang Wang, Wenming Li, Yuan Yao, Houtian Huang, Yutang Wang. A fine image motion compensation method for the panoramic TDI CCD camera in remote sensing applications. Optics Communications, 298-299 (2013).
21. Sebastian Petsch, Stefan Schuhladen, Lucas Dreesen，et al. The engineered eyeball, a tunable imaging system using soft-matter micro-optics. Light: Science&Applications, 5:e16068 (2016).
22. J. Kelly and G. S. Sukhatme, Visual-inertial simultaneous localization, mapping and sensor-to-sensor self-calibration in IEEE Int. Symp. on Computational Intelligence in Robotics and Automation, IEEE:360–368(2009).

Haipeng Kuang is a researcher in Changchun Institute of Optics Fine Mechanics and Physics ,and also a supervisor of postgraduate in the University of the Chinese Academy Of Sciences. he received his BS degree from the Jilin University of technology in 1994, and his MS degree from the University of the Chinese Academy of Science in 2000. he received his PhD. degree from the University of the Chinese Academy of Science in 2008. His current research interests include Optical Imaging and Mapping Techniques for Aerial Remote.

Lina Zheng is an associate researcher in Changchun Institute of Optics Fine Mechanics and Physics, and also a supervisor of postgraduate in the University of the Chinese Academy of Sciences. She received her BS degree in electronics from Jilin University in 2003, and her MS degree in mechatronics from the University of the Chinese Academy of Sciences in 2008. She received her PH.D degree in optical engineering from the University of the Chinese Academy of Sciences in 2013. Her current research interests include optical Imaging and mapping techniques for aerial remote camera.

Guoqin Yuan received his MS degree from Jilin University in 2007 and the PH.D degree in optical engineering from the University of the Chinese Academy of Sciences in 2012. He is now an associate researcher in Changchun Institute of Optics Fine Mechanics and Physics. His current research interests include optical Imaging and mapping techniques for aerial remote camera.

Jianjun Sun received his MS degree from Beihang University in 2012. He is now a research assistant in Changchun Institute of Optics Fine Mechanics and Physics. His current research interests include optical Imaging and mapping techniques for aerial remote camera.

Zhuang.Zhang received his B.S degree in applied physics from Hehai University in 2013. He is now an engineer in Changchun Institute of Optics, Fine Mechanics and Physics, Chinese Academy of Sciences. His current research interests include image processing and mapping techniques for aerial remote camera.